On the utilization of simplified methodologies for the wheel-rail contact

José Ferreira, Paulo Flores and Filipe Marques

Abstract. The utilization of multibody systems formulation allows to study the railway vehicle dynamics, as well study local damaging phenomena that occur in the wheel-rail interaction. However, the analysis of these phenomena requires long simulations to perform a significant prediction of their evolution. Having that in mind, the utilization of simplified approaches for the different steps of calculation of wheel-rail contact interaction are addressed, in particular, the utilization of planar or spatial approaches for the contact detection. Two parametric surfaces are used to describe both wheel and rail geometries, namely a revolution and an extruded body, respectively. Regarding the normal and tangential contact forces, an elastic approach is considered, therefore, these forces are treated as external forces acting on the multibody system and an Hertzian model with damping is employed for their evaluation. Finally, a trailer vehicle is considered as example of application to study different modeling strategies.

Key words: Wheel-Rail Contact, Railway Dynamics, Surfaces Definition, Multibody Dynamics.

José Ferreira
CMEMS-UMinho, Departamento de Engenharia Mecânica, Universidade do Minho, Campus de Azurém, Guimarães 4804-533, Portugal, e-mail: id9286@alunos.uminho.pt
Paulo Flores
CMEMS-UMinho, Departamento de Engenharia Mecânica, Universidade do Minho, Campus de Azurém, Guimarães 4804-533, Portugal, e-mail: pflores@dem.uminho.pt
Filipe Marques
CMEMS-UMinho, Departamento de Engenharia Mecânica, Universidade do Minho, Campus de Azurém, Guimarães 4804-533, Portugal, e-mail: fmarques@dem.uminho.pt

1 Introduction

The modeling of wheel-rail contact plays a preponderant role on the dynamic analysis of railway vehicles, since it represents the vehicle-track interaction where the developed forces are responsible for supporting and guiding the vehicle, as well as the traction and braking actions [1]. For an efficient multibody simulation of a railway vehicle, the methodology for assessing the wheel-rail contact forces has a critical importance, since it is often the bottleneck for achieving a lower simulation time [2]. This can be a critical issue when it is needed to perform long time simulations to predict the wheel-rail damaging phenomena, as wear or rolling contact fatigue [3]. There are several issues which might contribute for the improving of the numerical efficiency, namely, the contact detection methods [4], the integration algorithms, the degree of detail of the normal and creep force models [5], just to mention a few.

2 Wheel and rail geometric definition

The mathematical description of the wheel and rail profiles consists of a two-dimensional representation which can be extended to the three-dimensional space by defining their external surfaces. A bi-dimensional approach for the description of the wheel and rail has the advantage of allowing fast and straightforward numerical models but poses significant limitations regarding an accurate representation of the contact scenarios, as, for instance, in the presence of angular misalignments. Typically, the wheel and rail can be represented by two parametric surfaces [6], as represented in Fig. 1. The surface of each rail can be achieved through the sweep of its cross-section along a given path, in turn, the wheel surface is characterized as a revolution of its cross-section about its own axis. Since both cross-sections are defined as function of their lateral coordinate, each of these of surfaces can be described by two independent parameters, i.e., a point on the rail surface is defined by the lateral (u_r) and longitudinal (s_r) coordinates, and a point located on the wheel surface is given by its lateral (u_w) and angular (s_w) coordinates.

Based on the proposed surface parametrization, it is possible to write the equations that allow the determination of a location of given point on the wheel and on the rail as function of the surface parameters. Thus, following the representation of Fig. 1, the position of a point P on the rail surface is calculated as

$$\mathbf{r}_P^{side} = \mathbf{r}_\mathrm{r}^{side} + \mathbf{r}_{\mathrm{r},P}^{side} \tag{1}$$

where $\mathbf{r}_\mathrm{r}^{side}$ represents the location of the origin of the rail profile given as function of its arclength, and $\mathbf{r}_{\mathrm{r},P}^{side}$ expresses the distance vector from the rail origin and point *P*, which can be computed as

$$\mathbf{r}_{\mathrm{r},P}^{side} = \mathbf{A}_{\mathrm{r}}^{side} \begin{Bmatrix} 0 & u_{\mathrm{r},P}^{side} & f_{\mathrm{r},P}^{side} \end{Bmatrix}^{\mathrm{T}} \tag{2}$$

in which $f_{\mathrm{r},P}^{side}$ represents the ordinate of the rail profile, given as function of its lateral coordinate, as schematized in Fig. 2a, and $\mathbf{A}_{\mathrm{r}}^{side}$ denotes the rail transformation matrix and can defined as

$$\mathbf{A}_{\mathrm{r}}^{side} = \begin{bmatrix} \mathbf{t}_{\mathrm{r}}^{side} & \mathbf{n}_{\mathrm{r}}^{side} & \mathbf{b}_{\mathrm{r}}^{side} \end{bmatrix} \tag{3}$$

where $\mathbf{t}_{\mathrm{r}}^{side}$, $\mathbf{n}_{\mathrm{r}}^{side}$ and $\mathbf{b}_{\mathrm{r}}^{side}$ are the local tangent, normal and binormal vectors of the rail, respectively, and also given as function of its arclength.

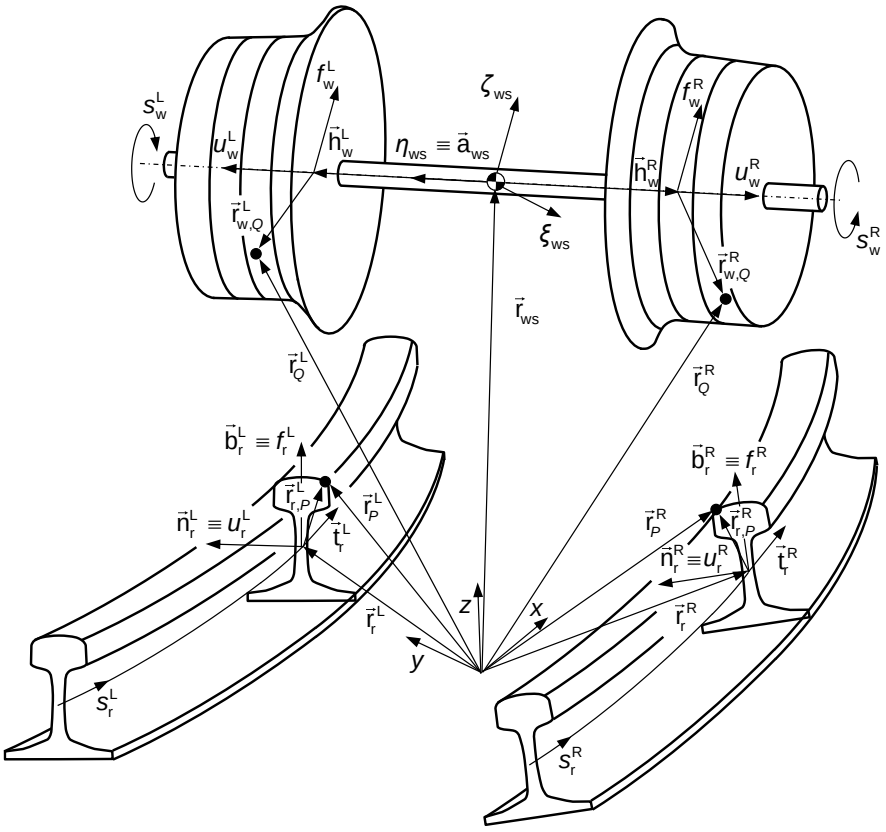

Fig. 1 Parametrization of the wheel and rail surfaces

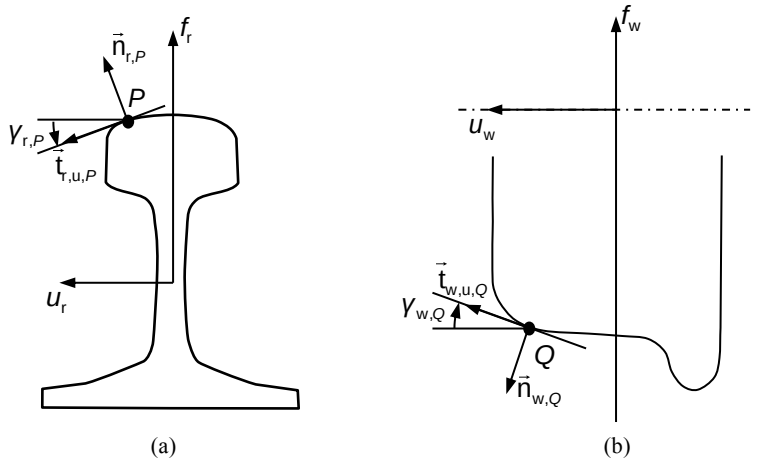

Fig. 2 Representation of an arbitrary point on (a) rail and (b) wheel profiles

In a similar manner, based on the representation of Fig. 1, the location of an arbitrary point Q on the wheel profile can be calculated as

$$\mathbf{r}_Q^{side} = \mathbf{r}_{\mathrm{ws}} + \mathbf{h}_{\mathrm{w}}^{side} + \mathbf{r}_{\mathrm{w},Q}^{side} \tag{4}$$

where $\mathbf{r}_{\mathrm{ws}}$ denotes location of the center of mass of the wheelset, $\mathbf{h}_{\mathrm{w}}^{side}$ represents a local position vector from the center of mass of the wheelset until the origin of the wheel profile defined to the left or right side accordingly, and $\mathbf{r}_{\mathrm{w},Q}^{side}$ expresses the distance vector from the wheel origin and point Q, given by the following expression

$$\mathbf{r}_{\mathrm{w},Q}^{side} = \mathbf{A}_{\mathrm{ws}} \mathbf{A}_{\mathrm{w,s}}^{side} \begin{Bmatrix} 0 & u_{\mathrm{w},Q}^{side} & f_{\mathrm{w},Q}^{side} \end{Bmatrix}^{\mathrm{T}} \tag{5}$$

in which $\mathbf{A}_{\mathrm{ws}}$ denotes the wheelset transformation matrix, $f_{\mathrm{w},Q}^{side}$ corresponds to the ordinate of the wheel profile which, similarly to the rail, is defined as function of its lateral coordinate, as represented in Fig. 2b, and $\mathbf{A}_{\mathrm{w,s}}^{side}$ is a transformation matrix that defines the rotation about the wheel axis, and it is computed differently for both sides as

$$\mathbf{A}_{\mathrm{w,s}}^{\mathrm{L}} = \begin{bmatrix} \cos\left(s_{\mathrm{w},Q}^{\mathrm{L}}\right) & 0 & \sin\left(s_{\mathrm{w},Q}^{\mathrm{L}}\right) \\ 0 & 1 & 0 \\ -\sin\left(s_{\mathrm{w},Q}^{\mathrm{L}}\right) & 0 & \cos\left(s_{\mathrm{w},Q}^{\mathrm{L}}\right) \end{bmatrix} \text{ or } \mathbf{A}_{\mathrm{w,s}}^{\mathrm{R}} = \begin{bmatrix} -\cos\left(s_{\mathrm{w},Q}^{\mathrm{R}}\right) & 0 & -\sin\left(s_{\mathrm{w},Q}^{\mathrm{R}}\right) \\ 0 & -1 & 0 \\ -\sin\left(s_{\mathrm{w},Q}^{\mathrm{R}}\right) & 0 & \cos\left(s_{\mathrm{w},Q}^{\mathrm{R}}\right) \end{bmatrix} \tag{6}$$

The definition of the normal and tangent vectors to the wheel and rail surfaces can be achieved using the derivative of the profiles functions as schematized in Fig. 2. Hence, the contact angle obtained from the profile data, which is typically given by a set of nodal points and, then, approximated by spline functions. These data can also be utilized to calculate the profile's local curvature which it is utilized to estimate the contact stiffness.

3 Contact detection

In this work, two methodologies for the identification of contact points are analyzed and compared. It must be noted that the definition of the surfaces' geometry described in the previous section is of paramount importance for the development and implementation of contact detection methodologies, as well as to enhance their efficiency and accuracy.

The first approach consists of a simplified methodology which performs the contact detection by the intersection between the 2D wheel and rail profiles, as illustrated in Fig. 3(a). Although the geometric parametrization of the contacting elements describes spatial surfaces, as shown in Section 2, this simplified approach searches the contact points through the comparison of the profiles position. First, the closest rail profile to the wheel is found, then the intersections between the rail profile at that position and the wheel transversal profile are identified and, finally, the maximum penetration in each contact patch is determined.

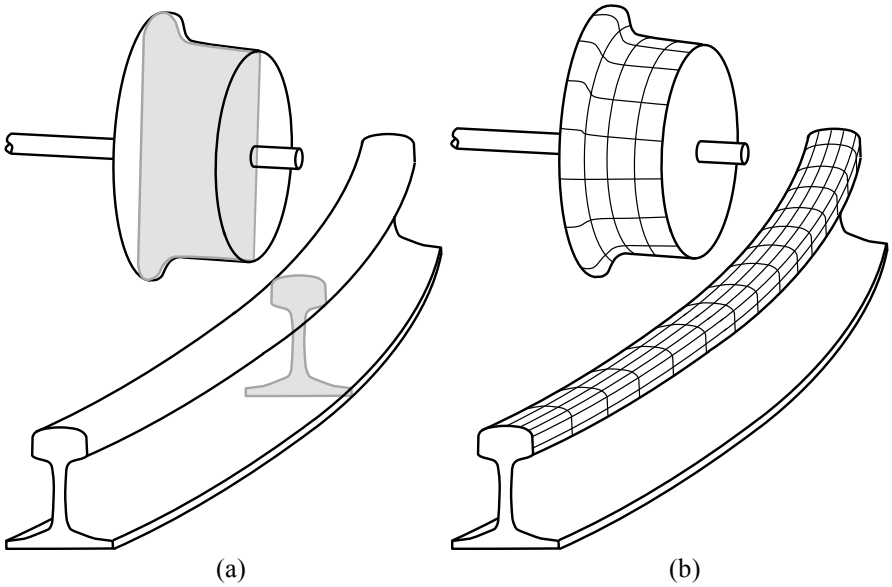

Fig. 3 Schematic representation of (a) bidimensional contact detection between wheel and rail profiles and (b) three-dimensional contact detection between wheel and rail surfaces

Alternatively, a spatial contact detection methodology is utilized to compare the perks of the utilization of these different procedures. In this method, the contact point can be located outside of the plane in which their planar profiles lie, as schematized in Fig. 3(b). This approach follows the methodologies developed by Marques et al. [8] in which the maximum penetration point is found by analyzing independently the strips of the wheel surface.

4 Contact force model

In this work, the normal contact force is estimated according to an Hertzian-based model which assumes elliptical contact area but considers a viscoelastic force-displacement behavior. Therefore, the normal force is computed as

$$f_{\mathrm{n}} = K\delta^{n} c_{\mathrm{d}} \tag{7}$$

where K expresses the generalized contact stiffness, which depends on the local contact geometry and material properties [8], δ is the pseudo-penetration or indentation between contacting surfaces, n defines the degree of nonlinearity of the model and it is 1.5 for metallic contacts, and c_{d} represents the damping factor calculated according to [9]. After the normal force evaluation, the size of the contact ellipse is determined using the local surfaces curvature.

Regarding the tangential or creep forces, a Lookup Table established from a contact patch parametrization with five input variables and computed based on CONTACT software is employed here [10, 11]. Although this approach was developed for simple double elliptical contact area, which is generally a non-Hertzian shape, it is adapted here for the Hertzian case.

5 Multibody systems formulation

The normal and tangential contact forces determined during the wheel and rail interaction are included in the dynamic equations of motion as external forces. Bearing that in mind, the equations of motion for a constrained multibody mechanical system can be formulated recurring to the Newton-Euler formulation with absolute or Cartesian coordinates together with the standard Lagrange multipliers technique [12]. In order to control the violation of the kinematic constraints, the Baumgarte stabilization technique is considered [13,14], and the system of equations of motion can be written in the following form

$$\begin{bmatrix} \mathbf{M} & \mathbf{D}^{\mathrm{T}} \\ \mathbf{D} & \mathbf{0} \end{bmatrix} \begin{Bmatrix} \dot{\mathbf{v}} \\ \boldsymbol{\lambda} \end{Bmatrix} = \begin{Bmatrix} \mathbf{g} \\ \boldsymbol{\gamma} - 2\alpha\dot{\boldsymbol{\Phi}} - \beta^{2}\boldsymbol{\Phi} \end{Bmatrix} \tag{8}$$

where **M** is the global mass or inertia matrix of the system, **D** denotes the Jacobian matrix of the constraints equations, $\dot{\mathbf{v}}$ represents the generalized accelerations vector, $\boldsymbol{\lambda}$ expresses the Lagrange multipliers vector, which represents the reaction forces and moments on the kinematic joints, **g** denotes the external generalized forces vector, in which the contact forces are included, $\boldsymbol{\gamma}$ is the commonly named right-hand side vector of acceleration constraints, $\boldsymbol{\Phi}$ and $\dot{\boldsymbol{\Phi}}$ denote the position and velocity constraints vectors, respectively, and α and β are positive constants that represent the feedback control parameters for the velocity and position constraints violation.

6 Example of application

A multibody model of a single wheelset running on a tangent track is utilized as example of application. In the beginning of the simulation, the wheelset has a lateral displacement of 2 mm to promote the hunting motion, and its initial velocity is 20 m/s. These dynamic simulations are performed in MATLAB code for spatial multibody dynamics, the simulation time is 10 s and the *ode45* algorithm is used for the time integration of the equations of motion. Figure 4 show the lateral motion of the wheelset using the 2D and 3D contact detection methods, which demonstrate equivalent results. The same interpretation can be made with the analysis of the contact point location on the wheel and rail profiles represented in Fig. 5. In terms of computational efficiency, the 2D detection method took around 90% of the computing time of 3D approach.

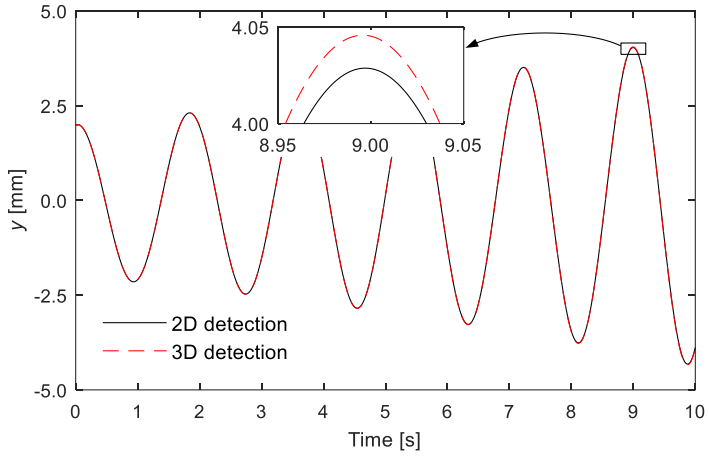

Fig. 4 Wheelset lateral position during the dynamic simulation

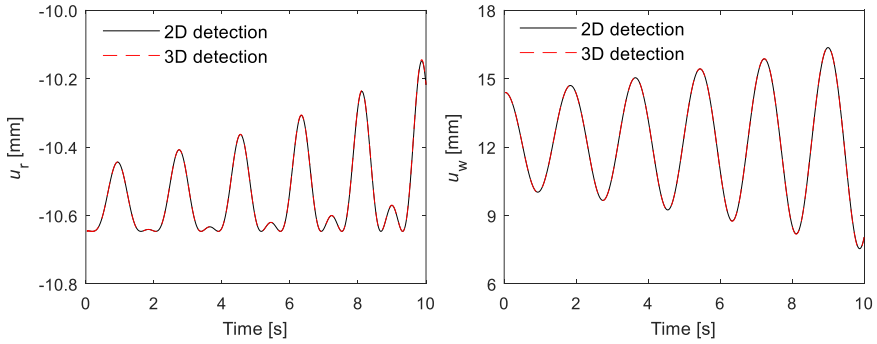

Fig. 5 Location of the contact points on the (a) rail and (b) wheel profiles

7 Conclusions

This work addresses the utilization of simplified methodologies on the evaluation of the forces developed on the wheel-rail contact interaction. For this purpose, two parametrized surfaces are employed for the definition of the contact geometries, and an Hertzian-based model is adopted for the normal and creep forces calculation. This allowed to study the impact of the modeling approaches on different running conditions. Further studies using different multibody models and running conditions will be addressed in the future to better understand the benefits and limitations of the utilization of simplified approaches on the wheel -rail contact modeling.

Acknowledgments This work has been supported by FCT with the reference project POCI-01-0145-FEDER-028424, by FEDER funds through the COMPETE 2020 - Programa Operacional Competi-tividade e Internacionalização. This work has been also supported by Portuguese Foundation for Science and Technology, under the national support to R&D units grant, with the reference project UIDB/04436/2020 and UIDP/04436/2020.

References

1. Meymand, S.Z., Keylin, A., Ahmadian, M.: A survey of wheel-rail contact models for rail vehicles. *Vehicle System Dynamics* **54**(3), 386-428 (2016)
2. Bruni, S., Meijaard, J.P., Rill, G., Schwab, A.L.: State-of-the-art and challenges of railway and road vehicle dynamics with multibody dynamics approaches. *Multibody System Dynamics* **49**(1), 1-32 (2020)
3. Soleimani, H., Moavenian, M.: Tribological Aspects of Wheel–Rail Contact: A Review of Wear Mechanisms and Effective Factors on Rolling Contact Fatigue. *Urban Rail Transit* **3**(4), 227-237 (2017)
4. Shabana, A.A., Tobaa, M., Sugiyama, H., Zaazaa, K.E.: On the computer formulations of the wheel/rail contact problem. *Nonlinear Dynamic*, **40**(2), 169-193 (2005)

5. Burgelman, N., Sichani, M.S., Enblom, R., Berg, M., Li, Z., Dollevoet, R.: Influence of wheel-rail contact modelling on vehicle dynamic simulation. *Vehicle System Dynamics* **53**(8), 1190-1203 (2015)
6. Pombo, J., Ambrósio, J., Silva, M.: A new wheel-rail contact model for railway dynamics. *Vehicle System Dynamics* **45**(2), 165-189 (2007)
7. Marques, F., Magalhães, H., Pombo, J., Ambrósio, J., Flores, P.: A three-dimensional approach for contact detection between realistic wheel and rail surfaces for improved railway dynamic analysis. Mechanism and Machine Theory, **149**, 103825 (2020)
8. Goldsmith, W.: Impact – The Theory and Physical Behaviour of Colliding Solids. Edward Arnold LTD London, United Kingdom (1960)
9. Ambrósio, J., Pombo, J.: A unified formulation for mechanical joints with and without clearances/bushings and/or stops in the framework of multibody systems. *Multibody System Dynamics* **42**(3), 317-345 (2018)
10. Piotrowski, J., Liu, B., Bruni, S.: The Kalker book of tables for non-Hertzian contact of wheel and rail. *Vehicle System Dynamics*, 55(6), 875-901 (2017)
11. Marques, F., Magalhães, H., Liu, B., Pombo, J., Flores, P., Ambrósio, J., Piotrowski, J., Bruni, S.: On the generation of enhanced lookup tables for wheel-rail contact models. *Wear*, 434-435, 202993 (2019)
12. Nikravesh, P.E.: Computer-Aided Analysis of Mechanical Systems. Prentice Hall, Engewood Cliffes (1988)
13. Baumgarte, J.: Stabilization of constraints and integrals of motion in dynamical systems. *Computer Methods in Applied Mechanics and Engineering* **1**(1), 1-16 (1972)
14. Marques, F., Souto, A.P., Flores, P.: On the constraints violation in forward dynamics of multibody systems. *Multibody System Dynamics* **39** (4), 385-419 (2017)